

# Developing the radium measurement system for JUNO's water Cherenkov detector

L.F. Xie<sup>a</sup>, J.C. Liu<sup>b</sup>, S.K. Qiu<sup>a</sup>, C. Guo<sup>b\*</sup>, Q. Tang<sup>a†</sup>, Y.P. Zhang<sup>b</sup>,  
P. Zhang<sup>b</sup>, C.G. Yang<sup>b</sup>,

<sup>a</sup> *School of Nuclear Science and Technology, University of South China, Hengyang, China*

<sup>b</sup> *Key Laboratory of Particle Astrophysics, Institute of High Energy Physics, Chinese Academy of Science, Beijing, China*

---

## Abstract

The Jiangmen Underground Neutrino Observatory(JUNO) is proposed to determine neutrino mass hierarchy using a 20 kton liquid scintillator detector. Strict radio-purity requirements have been put forward for all the components of the detector. One of the main background is the  $^{222}\text{Rn}$  dissolved in the water Cherenkov detector supposed to be less than 200 mBq/m<sup>3</sup> in JUNO.  $^{226}\text{Ra}$ , the progenitor of  $^{222}\text{Rn}$ , should also be taken seriously into account. In order to measure the radium concentration in water, a radium measurement system, which consists of the radium extracting system and the radium measurement system, has been developed. In this paper, the manufacture of Mn-fiber, which is the key part of radium extracting system, the calibration result of extracting efficiency as well as the measurement results of Daya Bay water samples will be presented.

*Keywords:* Radium, Radon, Mn-fiber

---

## 1. Introduction

The Jiangmen Underground Neutrino Observatory(JUNO), a multipurpose neutrino experiment, was proposed for neutrino mass hierarchy determination by detecting reactor antineutrinos from nuclear power plants as a

---

\*Corresponding author. Tel: +86-01088236256. E-mail address: guocong@ihep.ac.cn (C. Guo).

†Corresponding author. Tel: +86-13974753537. E-mail address: tangquan528@sina.com (Q. Tang).

primary physics goal [1]. The excellent energy resolution and large fiducial volume anticipates for the JUNO detector offer exciting opportunities for addressing many important topics in neutrino and astro-physics.

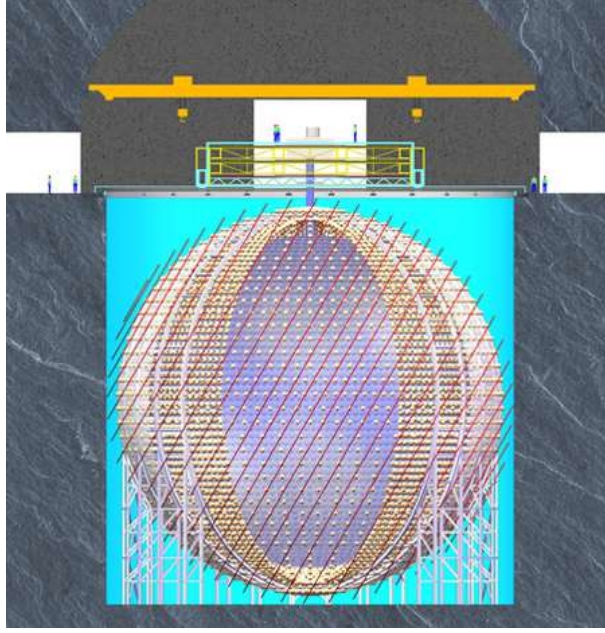


Figure 1: The designed schematic of JUNO detector.

JUNO consists of a central detector (CD) and a veto detector. The central detector, which contains 20 kton liquid scintillator,  $\sim 17000$  20 inch photomultiplier tubes (PMT) and 25600 3 inch PMTs, is designed to have a very good energy resolution of  $3\%/\sqrt{E(MeV)}$  and a long lifetime of over 20 years. The veto detector, which consists of a water Cherenkov detector and a muon tracker detector, is used for muon detection as well as muon induced background study and reduction. To suppress the radioactivity and cosmogenic background, the CD is submerged in the water Cherenkov detector, which is a pool filled with ultra-pure water and instrumented with  $\sim 2000$  20 inches microchannel plate photomultiplier tubes (MCP-PMTs). The top tracker (TT) from OPERA experiment will be placed on the top of the water Cherenkov detector to behave as a cosmic muon tracker.

The reactor electron antineutrino interacts with proton via the inverse  $\beta$ -decay (IBD) reaction in the liquid scintillator, resulting in a positron and a neutron. The positron, which carries the most kinetic energy of the neutrino,



where  $N_{Ra}(t)$  is the number of  $^{226}\text{Ra}$  atoms at time  $t$ ,  $N_{Ra}(0)$  is the initial number of  $^{226}\text{Ra}$  atoms,  $\lambda_{Ra}$  and  $\lambda_{Rn}$  are the decay constants of  $^{226}\text{Ra}$  and  $^{222}\text{Rn}$  respectively,  $N_{Rn}(t)$  is the number of  $^{222}\text{Rn}$  atoms at time  $t$ . The activity of  $^{222}\text{Rn}$  can be calculated as Eq. 3. Considering that  $^{226}\text{Ra}$  has a much longer half life than  $^{222}\text{Rn}$ , namely  $\lambda_{Ra} \ll \lambda_{Rn}$ , the transfer relation between  $^{226}\text{Ra}$  activity and  $^{222}\text{Rn}$  activity can be simplified to Eq. 4. Therefore, the activity of  $^{226}\text{Ra}$  can be easily gotten by measuring the emanated  $^{222}\text{Rn}$  activity.

$$\begin{aligned} A_{Rn}(t) &= \frac{dN_{Rn}(t)}{dt} \\ &= \lambda_{Ra}N_{Ra}(t) - \lambda_{Rn}N_{Rn}(t) \\ &= \frac{\lambda_{Ra}\lambda_{Rn}}{\lambda_{Rn} - \lambda_{Ra}}N_{Ra}(0)(e^{-\lambda_{Ra}t} - e^{-\lambda_{Rn}t}) \end{aligned} \quad (3)$$

$$A_{Ra}(t) = \frac{A_{Rn}(t)}{1 - e^{-\lambda_{Rn}t}} \quad (4)$$

### 3. Experimental setup

According to Ref. [3–6],  $MnO_2$ , which has strong adsorbability to radium, can be used to collect the dissolved radium ions in water. Considering the background level and radon emanation coefficient of the materials, acrylic fiber is chosen to be the carrier of  $MnO_2$ . The combination of acrylic fiber and  $MnO_2$  is called manganese fiber(Mn-fiber).

During the experiment, water flows through a column that contains Mn-fiber which could extract  $^{226}\text{Ra}$  from the flowing water [6–8]. After a certain amount of water has passed through the columns, the Mn-fiber are drained, removed and then sealed in an emanation chamber. The  $^{222}\text{Rn}$  from  $^{226}\text{Ra}$  decay is swept from the emanation chamber into an electrostatic chamber where it decays. The charged Po ions from the decay of Rn are carried by an electric field onto a Si-PIN where the  $\alpha$ s from  $^{214}\text{Po}$  and  $^{218}\text{Po}$  decay can be detected.

In this section, the manufacturing process of Mn-fiber, the extraction of radium from water as well as the measurement system will be presented.

### 3.1. Manufacture of Mn-fiber

Mn-fibers are made from acrylic fibers, potassium permanganate( $KMnO_4$ ) solution and concentrated sulfuric acid. The manufacture procedures and the ratio of the raw materials are as below:

A. Put 50 grams of acrylic fibers into 3 liters of 0.5 mol/L potassium permanganate solution and then pour in 30 ml concentrated sulfuric acid.

B. Heat to boiling and keep them boiling for  $\sim 2.5$  hours, during which the fibers should be properly stirred to make full contact with the solution.

C. Take out the fibers and keep rinsing them with distilled water until the water phase becomes light purple to remove the inefficiently adsorbed  $MnO_2$  and the attached  $KMnO_4$ .

D. Dry the fibers naturally in a clean room.

E. Keep sealed for use.

The pictures of acrylic fibers and dried Mn-fibers are shown in Fig. 3.



Figure 3: The real pictures of acrylic fibers and Mn-fibers.

### 3.2. Extracting radium from water

The dissolved radium in water will be adsorbed by  $MnO_2$  when the water flows over the column that contains Mn-fiber. Fig. 4 shows the real pictures

of the empty column and the using column. During the extracting stage, the sealing requirements for the containers are not strict because the radium content in air can be neglected and the tiny amount of radon adsorbed on the Mn-fibers will be removed at the measurement stage. As the right picture of Fig. 4 shows, some acrylic fibers are place on the top of the Mn-fibers to filter out the suspended particulate matters in the water. In order to eliminate the difference in adsorption efficiency caused by the different flow velocities, the water flow rate, which is controlled by a float flowmeter, is set to 250 ml/min during the experiment. Every 7.5 g Mn-fiber is used to extract the radium from every 30 L water.

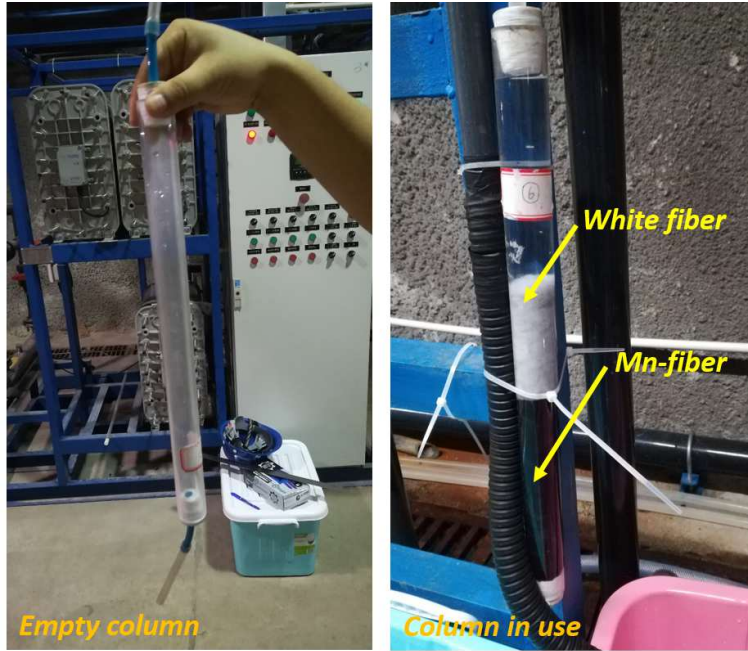


Figure 4: The real photographs of the column.

### 3.3. The measurement system

Fig. 5 shows the picture of the radium measurement system, which is updated based on the radon measurement system developed for JUNO prototype [9]. Compared with our previous work, the sensitivity of which was  $\sim 9$  mBq/m<sup>3</sup>, the calcium sulfate desiccant has been replaced with the low temperature dehumidification system, which consists of a dewar and a water container. During the experiment, the dewar is filled with cryogenic

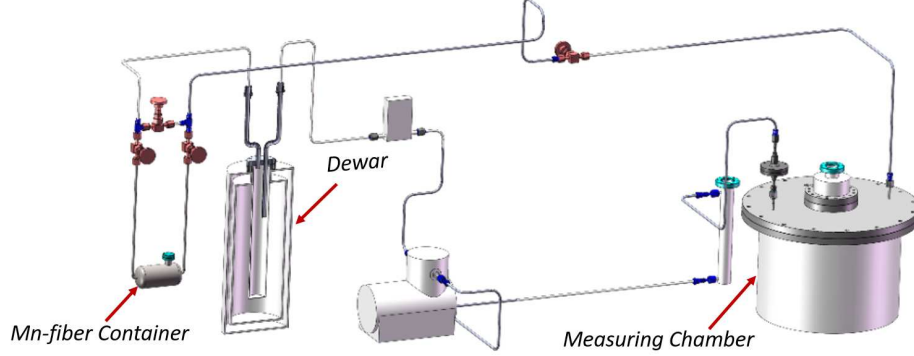


Figure 5: The scheme of the measuring system.

medium (low temperature nitrogen for example) to keep the inside at  $\sim -50$  centigrade, when the gas flows through the water container, heat exchanged between the gas and cryogenic medium, and the water vapor in the gas condenses, freezes and remains in the container. While the radon, which has much lower boiling point, will directly pass through the system. In our tests, the dehumidification module can keep the relative humidity of the system below 3%.

In our previous work, the  $\sim 9$  mBq/m<sup>3</sup> sensitivity was derived from the background measurement result, which is  $0.39 \pm 0.067$  counts/h. Our recent research shows that the background mainly comes from the residual air inside the detector. If the system is vacuum pumped and flushed with evaporated nitrogen for several times, the background level will be significantly reduced. In our last background measurement, only one event passed the selecting cuts for 137.5 hours data taking, which indicates that the sensitivity of the radon detector is  $\sim 1$  mBq/m<sup>3</sup> for one day measurement, the detail of the sensitivity estimation method can be found in ref [10].

In order to ensure the accuracy of radium concentration measurement, strict testing process has been developed.

A. Take out the Mn-fiber from the column, which is shown in the right part of Fig. 4, and put them into the Mn-fiber container of the measurement system, which is shown in Fig. 5. The Mn-fiber container is sealed with CF16 flange.

B. Pump the whole system to 100 Pa with a vacuum pump and then fill evaporative nitrogen into the system to atmospheric pressure. This process will be repeated for three times.

C. Isolate the Mn-fiber container.

D. Turn on the dehumidification module and circulate the other parts of the system for dehumidification until the relative humidity of the system down to 3%.

E. Keep the Mn-fiber container sealed for a period of time(at least 24 hours), during which the background measurement of the detector is carried out. The  $^{226}\text{Ra}$ , adsorbed by the  $\text{MnO}_2$ , will decay and its daughter,  $^{222}\text{Rn}$  will be accumulated in the Mn-fiber container during this period.

F. Transfer the gas in the Mn-fiber container into the measuring chamber with the pump and keep the circulation for more than 30 minutes so that the gas composition in the system is basically identical.

G. Dehumidify the whole system with the dehumidification module and do not start data taking until the relative humidity decreases to 3%.

H. Calculate the  $^{226}\text{Ra}$  concentration in water with Eq. 5.

$$C_{Ra} = \left( \frac{(n - n_b)V_s}{C_F(1 - e^{-\lambda_{Rn}t})} - mA_{bg} \right) / V_w \varepsilon \quad (5)$$

where  $C_{Ra}$  is the radium concentration in water in the unit of  $\text{mBq/m}^3$ ,  $n$  is the event rate of  $^{214}\text{Po}$  for the tested gas in procedure G,  $n_b$  is the  $^{214}\text{Po}$  event rate of the background, both  $n$  and  $n_b$  are in the unit of counts/h,  $V_s$  is the volume of the whole system in the unit of  $\text{m}^3$ ,  $C_F$  is the calibration factor of the radon detector in the unit of (counts/h)/( $\text{mBq/m}^3$ ),  $\lambda_{Rn}$  is the decay constant of  $^{222}\text{Rn}$ ,  $t$  is the sealing time of Mn-fiber in the unit of second,  $A_{bg}$  is the intrinsic radium background of Mn-fiber in the unit of  $\text{mBq/g}$ ,  $m$  is the mass of Mn-fiber in the unit of g,  $V_w$  is the volume of water in the unit of  $\text{m}^3$ ,  $\varepsilon$  is the radium extracting efficiency.

The  $\alpha$  signals from  $^{222}\text{Rn}$  decay are recorded with a LeCroy oscilloscope and the detail information of the readout system can be found in ref [9]. Fig. 6 shows the energy spectrum of  $^{222}\text{Rn}$  source as well as an example pulse of  $^{222}\text{Rn}$  signal.

#### 4. Calibration and measurement results

In order to get precise results, the intrinsic background and efficiency of whole system should be well studied. There are two sources of background, namely the background from radon detector, which will be measured before each sample measuring, and the intrinsic radium background of Mn-fiber, which should be measured once each batch because the raw materials and



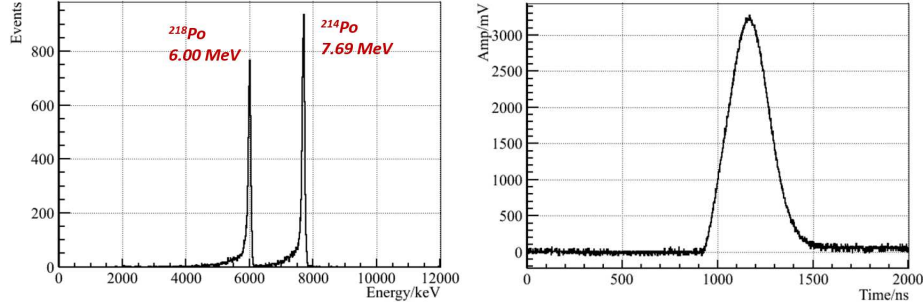


Figure 6: Left: The energy spectrum of  $^{222}\text{Rn}$  source. Right: An example pulse of  $^{222}\text{Rn}$  signal.

procedures of Mn-fiber manufacture may be slightly different and will result different radium intrinsic background of Mn-fibers. While for the efficiency, the detecting efficiency for  $\alpha$ s of the radon detector has been calibrated with a gas flow solid  $^{222}\text{Rn}$  source which is presented as  $C_F$  in Eq. 5. The radium extracting efficiency should also be calibrated each batch because the attachments may be oxidized differently, which results two forms of coatings, designated  $\text{MnO}_2$  and  $\text{MnO}_x$  (the incomplete oxidation), and the radium adsorption efficiency of them are slightly different [11]. Therefore, each batch of Mn-fibers has to be divided into three parts: the intrinsic background measuring part, the calibration part and the measurement part. The intrinsic background measurement has been carried out in accordance with the steps described in sec. 3.3 and the result is  $0.158 \pm 0.013$  mBq/g for the this batch, the error is statistical only.

#### 4.1. Calibration with radium solution

The radium extracting efficiency is calibrated with a known concentration radium solution, which is obtained by diluting 0.5 mL 12.4 mBq/mL radium solution with 30 L distilled water. The experiment was carried out in accordance with the steps described in sec. 3.2 and sec. 3.3. The energy spectrum of the background and the radium solution obtained by the detector are shown in Fig. 7 and the extracting efficiency,  $74.3\% \pm 14.5\%$ , is derived from the measured  $^{214}\text{Po}$  event rate with Eq. 5. The constants(const) in Eq. 5 are shown in Tab. 1 and the values(val) of the variables(var) for calibration in Eq. 5 are shown in Tab. 2. The error of  $C_{Ra}$  comes from the uncertainty of radium solution concentration, the errors of  $n$ ,  $n_b$  and  $C_F$  are statistical only and the errors of  $t$  and  $V$  are negligible compared with others.

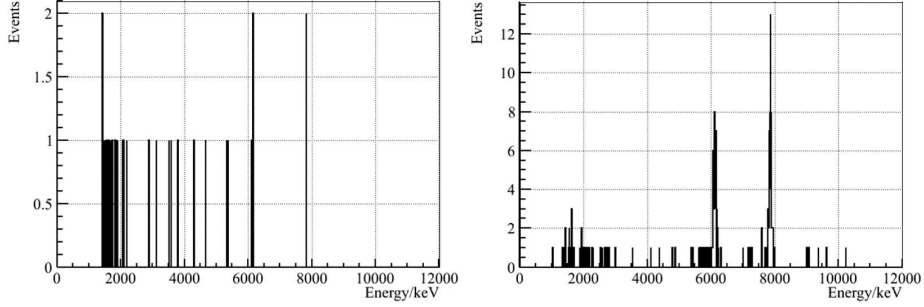


Figure 7: Left: The energy spectrum of background. Right: The energy spectrum of  $^{226}\text{Ra}$  solution. The data taking time of background and radium solution are 65.00 hours and 16.22 hours respectively.

Const	$V_s$	$C_F$	$\lambda_{Rn}$	m	$A_{bg}$	$V_w$
Val	0.035	$0.0264 \pm 0.0016$	$2.1e^{-6}$	7.5	$0.158 \pm 0.013$	0.03

Table 1: The values of the constants in Eq. 5.

#### 4.2. Measurement results

The radium concentration measurement system has been applied to the measurement of radium concentration in water of Daya Bay experiment hall 1(EH1) [13]. The Mn-fibers used in this measurement are in the same batch as those used for background measurement and extracting efficiency calibration, which are described in the previous chapter. The extracting procedures are carried out at the Daya Bay EH1 and the water samples are directly pumped out from the inner and outer pool. The measurements are carried out at the laboratory of Institute of High Energy Physics(IHEP). The measurement results, showing in Tab. 3, indicating that the ultra-pure water system at Daya Bay [12] also has effects on the removal of radium in water. For the Daya Bay experiment, the inner water pool and outer water pool share a set of water circulation and purification system, thus the average radium concentration at the inlet of the water system is  $422.2 \pm 182.5$  mBq/m<sup>3</sup>.

Var	$C_{Ra}(\text{mBq}/\text{m}^3)$	n	$n_b$	t(hour)	$\varepsilon$
Val	$210.0 \pm 21.0$	$4.32 \pm 0.52$	$0.03 \pm 0.02$	455.3	$74.3\% \pm 14.5\%$

Table 2: The values of the variables in Eq. 5 for calibration.

Therefore, the radium removal efficiency for the Daya Bay water system is  $80.3\% \pm 56.3\%$ .

Location	Outer Pool			
Var	n	$n_b$	t(hour)	$C_{Ra}(mBq/m^3)$
Val	$1.80 \pm 0.41$	$0.03 \pm 0.01$	29.5	$473.3 \pm 156.4$
Location	Inner Pool			
Var	n	$n_b$	t(hour)	$C_{Ra}(mBq/m^3)$
Val	$1.91 \pm 0.24$	$0.03 \pm 0.01$	40.7	$371.0 \pm 94.0$
Location	After the water purification system			
Var	n	$n_b$	t(hour)	$C_{Ra}(mBq/m^3)$
Val	$1.65 \pm 0.44$	$0.03 \pm 0.01$	161.4	$83.0 \pm 41.6$

Table 3: The measuring results of Daya Bay water samples.

## 5. Summary and Prospect

JUNO has put forward strict requirements on the radioactivity for all the components of the detector and according to the MC simulation results, the radon concentration in the water Cherenkov detector should be less than  $200 mBq/m^3$ .  $^{226}Ra$ , which is the progenitor of  $^{222}Rn$  and has a very long half life, should also be taken seriously into account. In order to measure the radium concentration in water, the measurement system, including the radium extracting system and the radon concentration measurement system, has been developed. The system has been used for measuring the radium concentration in water at Daya Bay and the radium concentration at different places of EH1 has been presented. The results also show that the ultra-pure water system of Daya Bay could remove  $\sim 80\%$  of the radium in water. For JUNO, the radium removing capability of the ultra-pure water system should also be well studied.

## 6. Acknowledgements

This work is supported by Strategic Priority Research Program of the Chinese Academy of Sciences (Grant No. XDA10010300), National Natural Science Foundation of China (Grant No. 11875280) and the Innovative Project of Institute of High Energy Physics (Grant No. Y9545140U2).

## References

## References

- [1] JUNO collaboration, J.Phys.G: Nucl.Part.Phys.43 030401(2016).
- [2] <http://atom.kaeri.re.kr:8080/ton/index.html>.
- [3] W.S. Moore, et al., J.Geophys.Res.78 (1973) 8880-8886;
- [4] W.S. Moore, et al., J.Geophys.Res.101 (1996) 1321-1329;
- [5] Jian-Xiong Wang, et al., Nucl.Instrum.Meth.A421:601-609(1999).
- [6] W.S. Moore, Deep-Sea Research 23 (1976) 647;
- [7] W.S. Moore, L.M. Cook, Nature 253 (1975) 262;
- [8] W.S. Moore, et al., J. Geophys. Res. 90 (1985) 6983.
- [9] Y.P. Zhang, et al., RDTM(2018)2:5;
- [10] Y.Nakano, et al., Nucl.Instrum.Meth.A 867, 108-114(2017).
- [11] T.C. Andersen, et al., Nucl.Instrum.Meth.A 501 (2003) 399-417.
- [12] J.Wilhelmi, et al., Journal of Water Process Engineering 5 (2015) 127-135.
- [13] Daya Bay Collaboration (F P. An et al.), Nucl. Instrum .Meth. A773 (2015) 8-20.